Available online at www.sciencedirect.com

ScienceDirect

Journal of Computational Physics 225 (2007) 2083–2097

JOURNAL OF COMPUTATIONAL PHYSICS

www.elsevier.com/locate/jcp

A characteristic-based shock-capturing scheme for hyperbolic problems

Tu Guo-Hua *, Yuan Xiang-Jiang

China Aerodynamics Research and Development Center, Mianyang 621000, PR China
National Laboratory for Computational Fluid Dynamics, Beijing 100083, PR China

Received 11 April 2006; received in revised form 18 December 2006; accepted 11 March 2007
Available online 24 March 2007

Abstract

In order to suppress numerical oscillations of linear compact schemes around discontinuities, a characteristic-based flux splitting limited method is introduced instead of ENO/WENO or other shock-capturing algorithms. This method begins with upwind schemes and flux vector splittings. The upwind schemes are projected along characteristic directions in a different way, and their amplitudes are carefully controlled by a special limiter in order to meet entropy condition and to prevent non-physical oscillations. A fifth-order linear compact upwind scheme is modified by this method for solving problems involving discontinuities. The properties of the numerical algorithm are checked on some benchmark problems in one, two and three space dimensions. Numerical results show that it is high-order accurate with high resolution and oscillation-free.

Keywords: High accuracy; High-order scheme; Shock-capturing; Compact scheme; Conservative differencing

1. Introduction

Direct numerical simulations (DNS) of turbulence and large-eddy simulations (LES) require the use of high accurate numerical schemes, which must be capable of resolving a very broad range of length scales that are often orders of magnitude apart [1]. It is generally believed that the accurate simulation of fluid flow with multiple and wide range of spatial scales and structures is a difficult task expect through spectral approximations. However, the use of spectral approximations is limited to simple geometries with generally periodic boundary conditions. Compact algorithm makes it possible to devise, on a given stencil, difference schemes that have much better resolution properties than conventional explicit difference schemes of comparable order of accuracy. Compact schemes with spectral-like resolution properties are more convenient to use than spectral and pseudo-spectral schemes, and are easier to handle, especially when non-trivial geometries are involved. The price paid is that one is required in general to invert a tri-diagonal system of linear algebra equation systems

* Corresponding author. Address: China Aerodynamics Research and Development Center, Mianyang 621000, PR China.
E-mail address: tootoo85@21cn.com (G.-H. Tu).

0021-9991/$ - see front matter
doi:10.1016/j.jcp.2007.03.007

to obtain derivatives. Central compact schemes have been developed from the 70s of the last century (see for instance [2,3]). However, centered algorithms are intrinsically non-dissipative, and cannot prevent odd–even decoupling, which gives rise to high frequency oscillations even in smooth regions. Reducing or removing such oscillations requires the introduction of dissipation terms. Asymmetric schemes with their dissipative properties are more stable. Fu and Ma [4], Adams and Shariff [5], Tolstykh and Lipavskii [6], Zhuang and Cheng [7] have developed some compact upwind (dissipative) schemes. These schemes enjoy high-order accuracy and high resolution for low wave numbers (large scale), while allowing much dissipation to high wave numbers (small scale), and the dissipation can be adjusted by a careful design. In general, compact upwind schemes can avoid odd–even decoupling and can prevent non-physical oscillations in smooth regions.

Recently, Chu and Fan [8] and Mahesh [9] have developed combined compact difference (CCD) schemes. Their ideas are basically to produce a high-order scheme by combining and solving the first and second derivatives together. The CCD schemes become more compact and more accurate than normal compact schemes. Finite-volume compact schemes have also been attempted by Gaitonde and Shang [10] and Kobayashi [11]. Nevertheless, in the transonic and supersonic flow regions when dealing with flows involving shock waves, one must use a numerical scheme which can both represent small scale structures with the minimum of numerical dissipation and capture discontinuities with the robustness that is common to Godunov-type methods. To achieve these dual objectives, high-order accurate shock-capturing schemes must be employed [12]. Unfortunately, the overall dependency characteristic of compact schemes hinders them from this purpose application, and the toughest difficulty is to capture the discontinuities smoothly in strong non-linear problems. Few attempts have been made to achieve the shock-capturing capability for compact schemes. Cockburn and Shu [13] have developed non-linearly stable compact schemes for shock calculations in 1994. They followed TVD's idea to define a non-linear limiter based on the local mean to avoid spurious oscillations while maintaining the formal accuracy of the schemes. However, spurious oscillations were still evident in their numerical test problems for their fourth-order scheme. An extended and improved version of Cockburn and Shu's scheme can be found in Yee's paper [14], but no numerical tests are given. Ravichandran [15] has employed a TVD limiter combined with kinetic flux vector splitting (KFVS) method to improve the stability of compact upwind schemes, and third-order schemes were given, which is supposed to degenerate to first-order accuracy at extrema. Deng and Zhang [16], Deng and Maekawa [17] have proposed some compact non-linear schemes by employing dissipative terms and weighted interpolations, but their schemes have lost the compactness (e.g. at least seven points are needed for their fifth-order schemes). Lerat and Corre [18] have employed residual-based dissipations to suppress non-physical oscillations, and a third-order compact scheme was given for compressible flows, but the scheme is only suitable for steady flows, and its applications to unsteady problems are in development. Ma and Fu [19] have developed high-order compact schemes with the method of group velocity control. Among all those efforts, blending compact schemes with other shock-capturing schemes such as ENO/WENO schemes is most common. ENO/WENO schemes [20–24] show great promise for accurately treating flow discontinuities. These schemes can be used to achieve a uniformly high-order accuracy while maintaining essentially non-oscillatory behavior for piecewise smooth functions by preventing the interpolation of the field values across the discontinuities as much as possible. This is done through a reconstruction or a flux evaluation procedure to allow the interpolating stencils to shift adaptively with the local smoothness of the function. However, the numerical solutions obtained with ENO/WENO schemes in smooth regions with moderately high field gradients are not very satisfactory (worse than padé schemes [30]). One way to eliminate this disadvantage of ENO/WENO schemes is to construct a hybrid scheme in which the scheme is switched to a conventional compact scheme in smooth regions and to an ENO/WENO scheme near/across discontinuities. However, a free threshold parameter, which controls the switch between the compact scheme and the ENO/WENO scheme, needs to be tuned, and some of the hybrid compact-ENO/WENO schemes [1,5] experience non-smooth transitions near the interfaces where the scheme switches types. Some spurious waves might be generated at these interfaces between different schemes, and these spurious waves would eventually propagate into the smooth regions as reported by Adams and Shariff [5]. Ren et al. [25] have developed characteristic-wise hybrid compact-WENO schemes, which can be regarded as an improvement of the scheme presented in [1].

As pointed by Titarev and Toro [26], the design of high-order accurate numerical schemes for hyperbolic conservation laws is a formidable task since three major difficulties have to be overcome: ensuring the conservation property, preserving the high order of accuracy in both time and space, and controlling the generation of spurious oscillations in vicinity of discontinuities. In the present study, we try to overcome the difficulties except the accuracy in time. Unlike the discontinuity-capturing methods mentioned above, a new characteristic-based method is proposed to surmount the shortcomings of high-order linear compact schemes. The organization of the paper is as follows: In Section 2, the characteristic-based method is given to suppress spurious oscillations of linear upwind schemes which are applied to get an approximation of the first spatial derivatives, and a shock-capturing scheme is formulated based on a fifth-order linear compact upwind scheme. Some numerical test cases in one-dimensional and multi-dimensional Euler systems are presented and discussed in Section 3, including some comparisons with other high-order schemes, and the results show that the characteristic-based shock-capturing compact scheme possesses the merits of the linear compact scheme, e.g. spectral-like resolution, higher-order accuracy, etc. Finally, concluding remarks are provided in Section 4.

2. Characteristic-based shock-capturing method

2.1. Characteristic-based treatment

Consider a hyperbolic system of conservation laws

$$\frac{\partial Q}{\partial t}+\frac{\partial F(Q)}{\partial x}=0 \tag{1}$$

or its non-conservative form

$$\frac{\partial Q}{\partial t}+A\frac{\partial Q}{\partial x}=0 \tag{2}$$

where $A=\partial F/\partial Q$, and all the eigenvalues $\lambda^{(k)}$ of A are real numbers. Let L and R be the left and right eigenvector matrices of A, then $A=R\Lambda L, R=L^{-1}$ and Λ is the diagonal matrix of $\lambda^{(k)}$.

Let us discrete the space into uniform intervals of size Δx, and various quantities at x_i will be identified by the subscript i. No matter what kind of algorithms are employed, the semi-discretize scheme of Eq. (1) can be written as

$$\left(\frac{\mathrm{d}Q}{\mathrm{d}t}\right)_i=-\frac{(H^+_{i+1/2}+H^-_{i+1/2})-(H^+_{i-1/2}+H^-_{i-1/2})}{\Delta x_i} \tag{3}$$

where $H^\pm_{i+1/2}$ can be regarded as the negative/positive numerical flux at an interface between two conterminous cells, and different schemes will give different definitions for them.

The flux F of Eq. (1) can be split by a flux vector splitting method (in this paper, Steger–Warming splitting), and $F=F^++F^-$ such that $F^\pm_i$ can be regarded as the average positive/negative fluxes in the ith grid cell. Then $H^+_{i+1/2}-F^+_i$ and $F^-_{i+1}-H^-_{i+1/2}$ indicate the flowing status of the fluxes. Let us project the flowing fluxes along characteristic directions by defining

$$\Delta\mathscr{W}^+_{i+1/2}=L^{\mathrm{l}}_{i+1/2}(H^+_{i+1/2}-F^+_i),\quad \Delta\mathscr{W}^-_{i+1/2}=L^{\mathrm{r}}_{i+1/2}(F^-_{i+1}-H^-_{i+1/2}) \tag{4}$$

where $L^{\mathrm{l}}_{i+1/2}$and $L^{\mathrm{r}}_{i+1/2}$ are the left eigenvector matrices of $A^{\mathrm{l}}_{i+1/2}$ and $A^{\mathrm{r}}_{i+1/2}$, respectively. The right eigenvector matrices $R^{\mathrm{l}}_{i+1/2}=(L^{\mathrm{l}}_{i+1/2})^{-1}$ and $R^{\mathrm{r}}_{i+1/2}=(L^{\mathrm{r}}_{i+1/2})^{-1}$. The definition of $A^{\mathrm{l}}_{i+1/2}$ and $A^{\mathrm{r}}_{i+1/2}$ will be given later.

$\mathscr{W}^\pm_{i+1/2}$ are similar to the characteristic variables, and their difference form, $\Delta\mathscr{W}^\pm_{i+1/2}$, are related to the amplitudes of the characteristic waves. When the same class of characteristics intersects, according to entropy criterion, some information must be lost with intersecting characteristics, namely, the amplitudes of the characteristic waves decrease non-linearly. Furthermore, non-physical solutions (spurious oscillations) may appear in flow fields even though no intersecting characteristics taking place. So, some kind of limiter function φ should be formulated to describe the damping phenomenon and prevent non-physical oscillations. The modified characteristic decompositions are

$$\delta\mathscr{W}^+_{i+1/2}=\varphi(\Delta\mathscr{W}^+_{i+1/2},\Delta\hat{\mathscr{W}}^+_{i+1/2},\Delta\hat{\mathscr{W}}^+_{i-1/2}),\quad \delta\mathscr{W}^-_{i+1/2}=\varphi(\Delta\mathscr{W}^-_{i+1/2},\Delta\hat{\mathscr{W}}^-_{i+1/2},\Delta\hat{\mathscr{W}}^-_{i+3/2}) \tag{5}$$

where φ is a limiter and $\Delta\hat{\mathscr{W}}^{+}_{i+1/2} = L^{\mathrm{l}}_{i+1/2}(F^{+}_{i+1} - F^{+}_{i}), \Delta\hat{\mathscr{W}}^{-}_{i+1/2} = L^{\mathrm{r}}_{i+1/2}(F^{-}_{i+1} - F^{-}_{i})$, are the coarse approximations of the flowing fluxes in the characteristic directions. Eq. (5) is similar to Eq. (2.12) of [15], the differences being the limiter and the premultiplication of flux differences by the left eigenvector matrix.

In this paper, we use the second limiter listed in [27]

$$\varphi(a,b,c) = \begin{cases} \operatorname{sign}(a)\cdot\min\left(|a|,|b|,\frac{2bc}{|a|+|c|+\varepsilon}\right) & \text{if } a, b \text{ and } c \text{ have the same sign} \\ 0 \quad \text{others} \end{cases} \tag{6}$$

where a, b and c are the three components in Eq. (5), respectively, which are non-exchangeable, and $\varepsilon \to 0$ is a small positive parameter employed to avoid division by zero. Our experiences show that it has no effect on the accuracy if it is less than 1E−7. In this paper, ε = 1E−9.

Now, the scheme can be converted back to conservative form:

$$\overline{H}^{+}_{i+1/2} = F^{+}_{i} + R^{\mathrm{l}}_{i+1/2}\delta\mathscr{W}^{+}_{i+1/2}, \quad \overline{H}^{-}_{i+1/2} = F^{-}_{i+1} - R^{\mathrm{r}}_{i+1/2}\delta\mathscr{W}^{-}_{i+1/2} \tag{7}$$

Then the modified semi-discretize scheme can be given by

$$\left(\frac{\mathrm{d}Q}{\mathrm{d}t}\right)_i = -\frac{(\overline{H}^{+}_{i+1/2} + \overline{H}^{-}_{i+1/2}) - (\overline{H}^{+}_{i-1/2} + \overline{H}^{-}_{i-1/2})}{\Delta x_i} \tag{8}$$

Eq. (8) is the characteristic-based shock-capturing scheme. It benefits from the following mature techniques: upwind method and flux splitting, characteristic decomposition, and limiters which are widely used in TVD schemes.

2.2. Choosing $A^{\mathrm{l}}_{i+1/2}$ and $A^{\mathrm{r}}_{i+1/2}$

A natural choice is $A^{\mathrm{l}}_{i+1/2} = A^{\mathrm{r}}_{i+1/2} = A_{i+1/2}$ at each fixed $x_{i+1/2}$. $A_{i+1/2}$ can be calculated by a simple arithmetical mean, or Roe average, of A_j and A_{j+1}. However, we propose $A^{\mathrm{l}}_{i+1/2} = A_i = A(Q_i)$ and $A^{\mathrm{r}}_{i+1/2} = A_{i+1} = A(Q_{i+1})$, which is more convenient and stable. After every given $A^{\mathrm{l}}_{i+1/2}$ and $A^{\mathrm{r}}_{i+1/2}$, their left and right eigenvector matrices are obvious, for example $L^{\mathrm{l}}_{i+1/2} = L(Q_i)$ and $L^{\mathrm{r}}_{i+1/2} = L(Q_{i+1})$.

Numerical tests show that the difference of the definition of $A^{\mathrm{l}}_{i+1/2}$ and $A^{\mathrm{r}}_{i+1/2}$ has little influence on the numerical solutions. The main reason may be that $A^{\mathrm{l}}_{i+1/2}$ and $A^{\mathrm{r}}_{i+1/2}$ do not appear explicitly, and their left and right eigenvector matrices appear together. Namely, the left eigenvector matrices are used to project the variables along the characteristic directions, and their corresponding right eigenvector matrices are used to convert the limited components back into their original forms.

2.3. A fifth-order upwind compact scheme

$H^{\pm}_{j+1/2}$ (In Eqs. (3) and (4)) can be acquired by many high-order schemes. Because compact schemes possess the merits of spectral-like resolution, higher-order accuracy in fewer grid stencils, and easier for boundary closure, a fifth-order linear compact upwind scheme is cited.

$$9H^{+}_{i-1/2} + 18H^{+}_{i+1/2} + 3H^{+}_{i+3/2} = 10F^{+}_{i+1} + 19F^{+}_{i} + F^{+}_{i-1} \tag{9a}$$

$$3H^{-}_{i-1/2} + 18H^{-}_{i+1/2} + 9H^{-}_{i+3/2} = F^{-}_{i+2} + 19F^{-}_{i+1} + 10F^{-}_{i} \tag{9b}$$

The fifth-order compact scheme has also been used by many other authors, e.g. [1,25]. Pirozzoli [1] has also made a detailed analysis of the scheme, and the results show its excellent resolution properties. It is clear that the linear compact schemes will cause non-physical oscillations (Gibbs phenomena) when they are applied directly to flow with discontinuities, and the oscillations do not decay when the grid is refined. In this case, we can modify the linear scheme by the method given in 2.1. It is evident that the linear compact scheme is based on four-grid stencils and the characteristic-based method does not extend the stencils. The steps for the method are

(1) Solve Eq. (9) for $H^{\pm}_{i+1/2}$ (linear compact scheme);
(2) Solve Eq. (4) for $\Delta\mathscr{W}^{\pm}_{i+1/2}$ (project onto the characteristic fields);

(3) Solve Eq. (5) for $\delta\mathscr{W}^{\pm}_{i+1/2}$ with the limiter (6) (limiting the projected components);
(4) Solve Eq. (7) for $\overline{H}^{\pm}_{i+1/2}$ (project back) and get the semi-discretize scheme (8).

2.4. Extension to multi-dimensions in general coordinates

The Euler equations in three-dimensional general coordinate system may be written as

$$\frac{\partial \widetilde{Q}}{\partial t} + \frac{\partial F^{\xi}}{\partial \xi} + \frac{\partial F^{\eta}}{\partial \eta} + \frac{\partial F^{\zeta}}{\partial \zeta} = 0 \tag{10}$$

where the superscripts ξ, η and ζ denote the variables in ξ, η and ζ directions, respectively, and

$$\begin{aligned}
\widetilde{Q} &= Q/J \\
F^{\xi} &= (\xi_x F^x + \xi_y F^y + \xi_z F^z)/J \\
F^{\eta} &= (\eta_x F^x + \eta_y F^y + \eta_z F^z)/J \\
F^{\zeta} &= (\zeta_x F^x + \zeta_y F^y + \zeta_z F^z)/J
\end{aligned}$$

Q denotes the conservative variables. F^x, F^y and F^z are the flux vectors in x, y and z directions, respectively. J is the Jacobian of the transformation.

The proposed shock-capturing scheme is subsequently achieved by using the reconstruction relations for the ξ, η and ζ directions separately. For example, in the ξ direction, let $A^{\xi} = \partial F^{\xi}/\partial \widetilde{Q}, L^{\xi}$ and R^{ξ} be the left and right eigenvector matrices of $A^{\xi}, F_i^{\xi+}$ and $F_i^{\xi-}$ be the splittings of F_i^{ξ}, if we replace, in Eqs. (4)–(7) and (9), $H^{\pm}_{i+1/2}$ with $H^{\xi\pm}_{i+1/2}, F_i^{\pm}$ with $F_i^{\xi\pm}, L^1_{i+1/2}$ with $L^{\xi 1}_{i+1/2}$, and so forth, we can get the discretization of $\partial F^{\xi}/\partial \xi$

$$\left(\frac{\partial F^{\xi}}{\partial \xi}\right)_i = \frac{(\overline{H}^{\xi+}_{i+1/2} + \overline{H}^{\xi-}_{i+1/2}) - (\overline{H}^{\xi+}_{i-1/2} + \overline{H}^{\xi-}_{i-1/2})}{\Delta \xi_i} \tag{11}$$

The semi-discretization of Eq. (10) can be given by

$$\begin{aligned}
\left(\frac{\mathrm{d}\widetilde{Q}}{\mathrm{d}t}\right)_{i,j,k} = &-\frac{\overline{H}^{\xi+}_{i+1/2,j,k} + \overline{H}^{\xi-}_{i+1/2,j,k} - \overline{H}^{\xi+}_{i-1/2,j,k} - \overline{H}^{\xi-}_{i-1/2,j,k}}{\Delta \xi_{i,j,k}} - \frac{\overline{H}^{\eta+}_{i,j+1/2,k} + \overline{H}^{\eta-}_{i,j+1/2,k} - \overline{H}^{\eta+}_{i,j-1/2,k} - \overline{H}^{\eta-}_{i,j-1/2,k}}{\Delta \eta_{i,j,k}} \\
&- \frac{\overline{H}^{\zeta+}_{i,j,k+1/2} + \overline{H}^{\zeta-}_{i,j,k+1/2} - \overline{H}^{\zeta+}_{i,j,k-1/2} - \overline{H}^{\zeta-}_{i,j,k-1/2}}{\Delta \xi_{i,j,k}}
\end{aligned} \tag{12}$$

where the subscripts i, j and k denote the positions in the ξ, η and ζ directions, respectively.

In the following sections, we will discuss the application of the characteristic-based conservative compact scheme (denoted by CC5-C-B) for some benchmark cases in one, two and three dimensions.

3. Numerical tests

For the motion of inviscid compressible fluids, the elements in Eq. (1) are

$$Q = [\rho, \rho\vec{u}, \rho e], \quad F = [\mathrm{div}(\rho\vec{u}), \mathrm{div}(\rho\vec{u} \otimes \vec{u}) + \nabla p, \mathrm{div}(\rho e\vec{u} + p\vec{u})]$$

where ρ is the fluid density, $\vec{u}$ is the velocity and e is the total energy, defined as the sum of the internal energy plus the kinetic energy. The system is closed by defining the pressure p through the equation of state for a perfect gas, $p = \rho e(\gamma - 1)$, where the constant γ is the ratio of specific heats. In all our tests considered, $\gamma = 1.4$.

In this paper, the temporal derivative is discretized by the third-order TVD type Runge–Kutta method presented in [21]

3.1. 1D Euler system

3.1.1. Lax shock tube

The first test case is the Riemann problem proposed by Lax. The initial condition is $(\rho, u, p)_L = (0.445, 0.698, 3.528)$ and $(\rho, u, p)_R = (0.5, 0, 0.571)$. We have computed the solution up to $t = 0.8$ with 100 cells. The results are shown in Fig. 1. It can be observed that the accuracy of the CC5-C-B scheme is comparable to the OSMP7 scheme [12], and the result of CC5-C-B is better than that of WENO-RF-5 (fifth order [28]). The WENO-RF-5 and other WENO schemes in [22,28] are more diffusive around the discontinuities than the CC5-C-B scheme is. We would like to point out that, according to our experience and [12,28], this case is demanding of the robustness of schemes because the shock wave is rather strong, and oscillations can appear for some non-characteristic-based schemes.

3.1.2. Shock-wave interacting with a density disturbance

In the previous test case, we have shown the good shock-capturing capability and robustness of the CC5-C-B scheme. As it is well known, limiters will degenerate the accuracy at extrema, we will check out how the scheme performs at extrema by calculating the problem of a shock-wave interaction. In this test (also called Shu–Osher problem), which was proposed in [22], a moving Mach 3 shock interacts with a sinusoidal density profile. The 1D Euler equations are solved on the spatial domain $x \in [-5, 5]$. The initial condition is

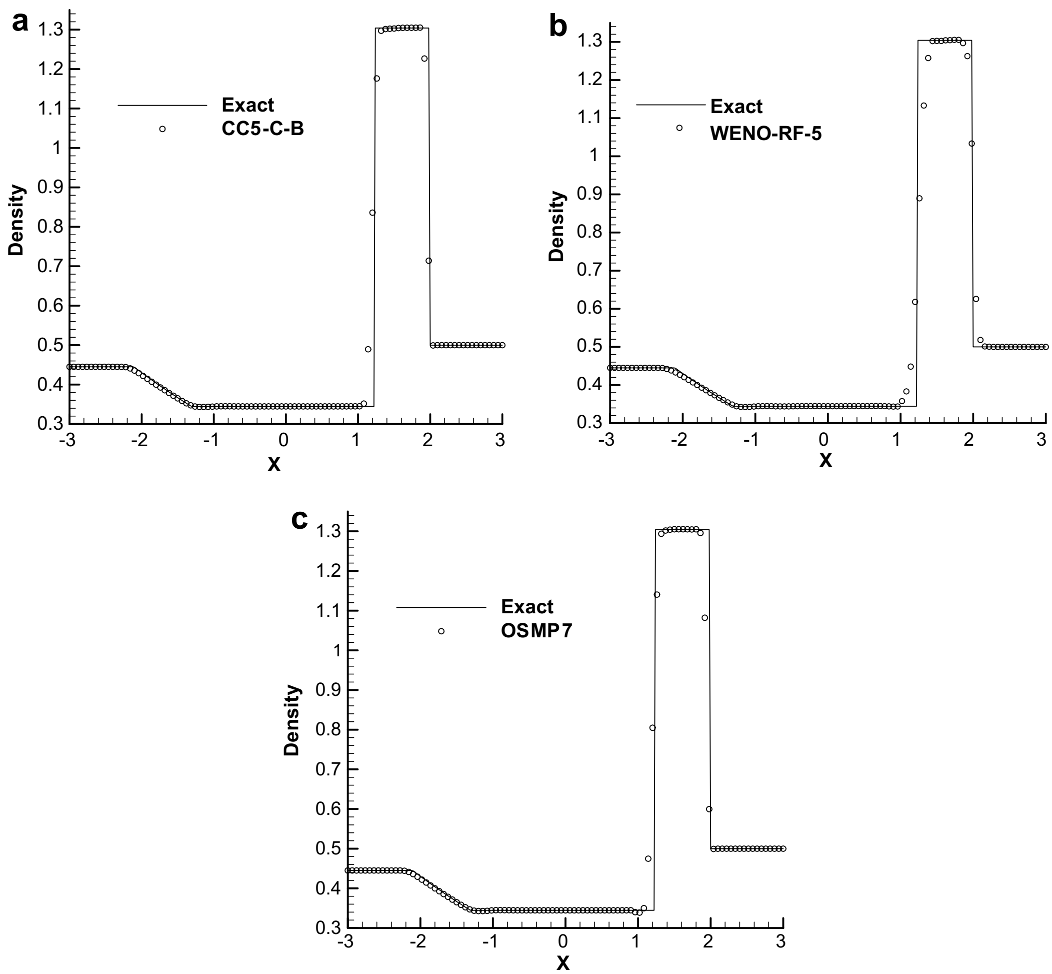

Fig. 1. Density distributions for the Lax test: (a) The fifth-order characteristic-based conservative compact scheme (CC5-C-B); (b) The fifth-order WENO scheme presented in [28]; (c) The seventh-order OSMP scheme presented in [12].

$$(\rho, u, p) = \begin{cases} (3.857143, 2.629369, 10.3333333) & \text{if } x \leqslant -4 \\ (1 + 0.2\sin(5x), 0, 1) & \text{if } x > -4 \end{cases}$$

The solution is advanced in time up to $t = 1.8$. The computed density fields are reported in Fig. 2, in which the solids lines are grid independent solutions. By comparing Fig. 2(b) with (c) and (d), it can be found that the CC5-C-B scheme gives much better resolution than the third-order compact-TVD scheme [15] does, and the limiter (6) holds higher accuracy than the minmod limiter does. By further comparing Fig. 2(a) with the results in [1], where the fifth-order WENO (Fig. 10, W5), the seventh-order WENO (Fig. 10, W7) and the hybrid compact-WENO (Fig. 10, H5 and H7) schemes are used for the calculations, we can find the following differences: (1) The CC5-C-B scheme gives better resolution for both the acoustic waves and the entropy waves than that of the fifth-order WENO schemes. (2) The hybrid schemes give the highest resolution for the entropy waves, but, (3) there are some oscillations in their solutions. (4) The CC5-C-B scheme gives the best solution for the acoustic waves.

3.1.3. A convergence test

In the previous test cases, the robustness, good shock-capturing capability and high resolving power of the CC5-C-B scheme have been shown. In this test case, attentions are focused on its performance in a smooth region which contains a density disturbance. The initial condition is $(\rho, u, p) = (1 + 0.2\sin(x), 1, 1)$. The exact solution is $(\rho, u, p) = (1 + 0.2\sin(x - t), 1, 1)$. The computational domain is taken to be $[0, 2\pi]$ with periodic

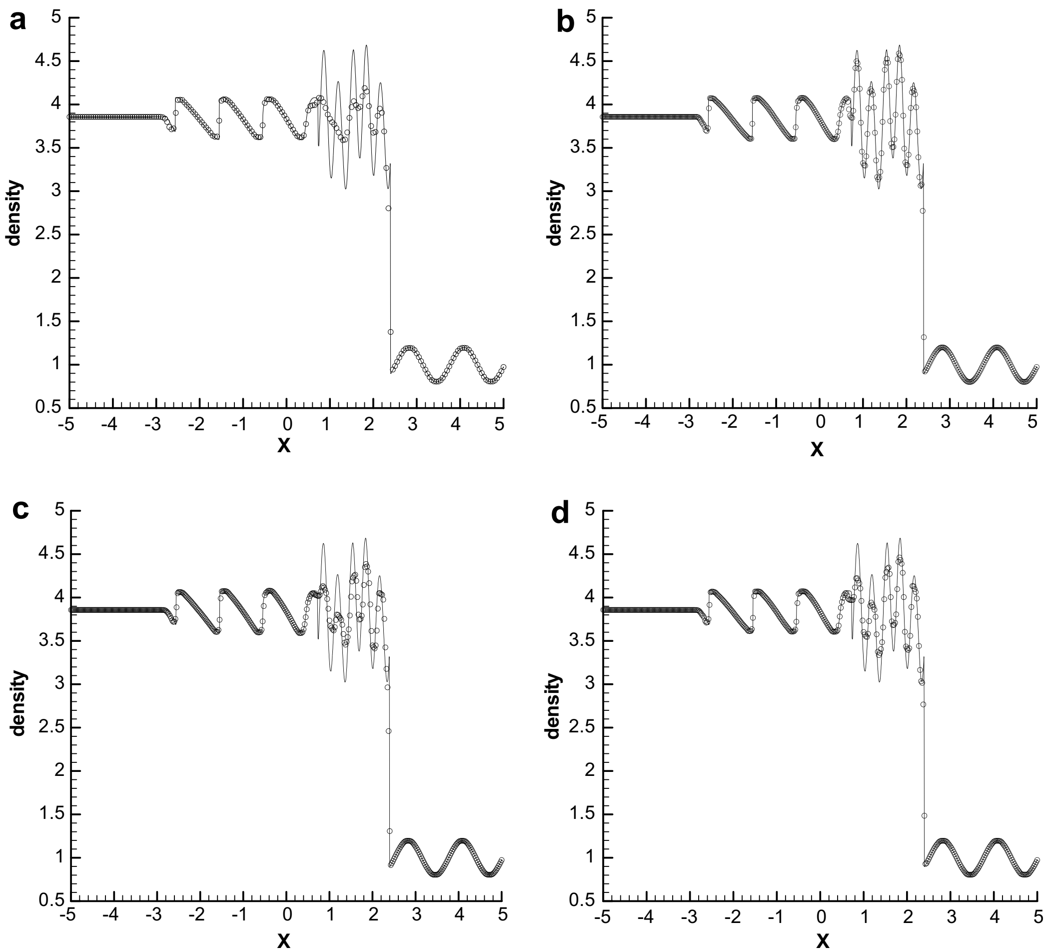

Fig. 2. Solutions of the Shu–Osher problem at $t = 0.18$. (a) CC5-C-B, 200 cells; (b) CC5-C-B, 400 cells; (c) Third-order compact-TVD [15], 400 cells; (d) Fifth-order compact scheme with minmod limiter, 400 cells.

boundary conditions. A uniformly spaced grid has been used with a time step which is varied with the grid length h, $\Delta t = h^3$, so as to rule out the time discretization error. The solution has been advanced in time up to $t = 2$. The convergence evaluation is shown in Fig. 3. For reference purposes, the lines with N^{-4} (solid) and N^{-5} (dashed) slopes are also shown. The figure indicates that the asymptotic convergence rate of the CC5-C-B scheme on coarse grids is similar to N^{-4}. However, on fined meshes ($N > 85$), the convergence rate is slightly slower than N^{-4}. As shown in [1], the convergence rate of the linear compact scheme is N^{-5}. In order to check out the reason of the slow convergence rate of the CC5-C-B scheme, we show in Fig. 4 the computed solution of density and its error. It can be found that the dominated errors appear near the extrema where $\Delta\rho$ changes its sign. Therefore the limier (6) will make the CC5-C-B scheme to deviate away from the linear compact scheme. Since the limier (6) is necessary for discontinuities-capturing, a way to mitigate the disadvantage of the CC5-C-B scheme is to turn off the limiter in smooth regions (such as the subsonic region of a boundary flow).

3.2. 2D Euler system

3.2.1. 2D Riemann problems

Following the notation introduced in [29], the results were obtained for configuration 5 and configuration 16. The initial conditions for configuration 5 and configuration 16 are shown in Fig. 5. Two sets of grid are tested, one is 200×200, and the other is 400×400.

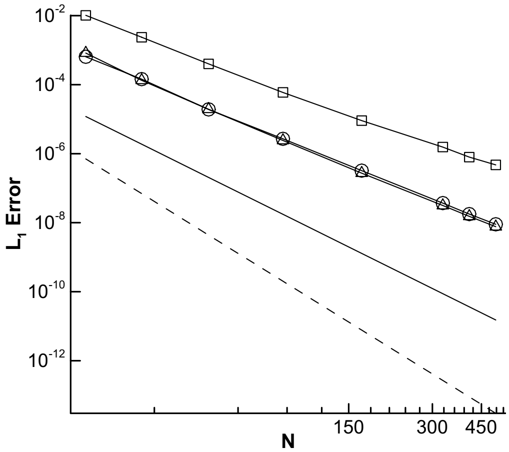

Fig. 3. Convergence test. □: L_1 error of ρ, △: L_1 error of u, ○: L_1 error of p.

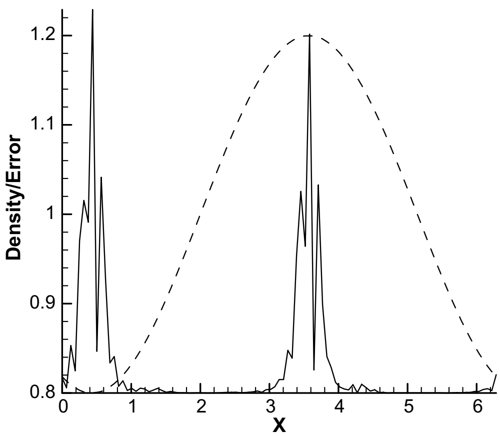

Fig. 4. Distribution of computed ρ and errors. Solid: $0.8 + 1000|\rho - \rho_e|$, dashed: ρ.

Fig. 5

Fig. 11

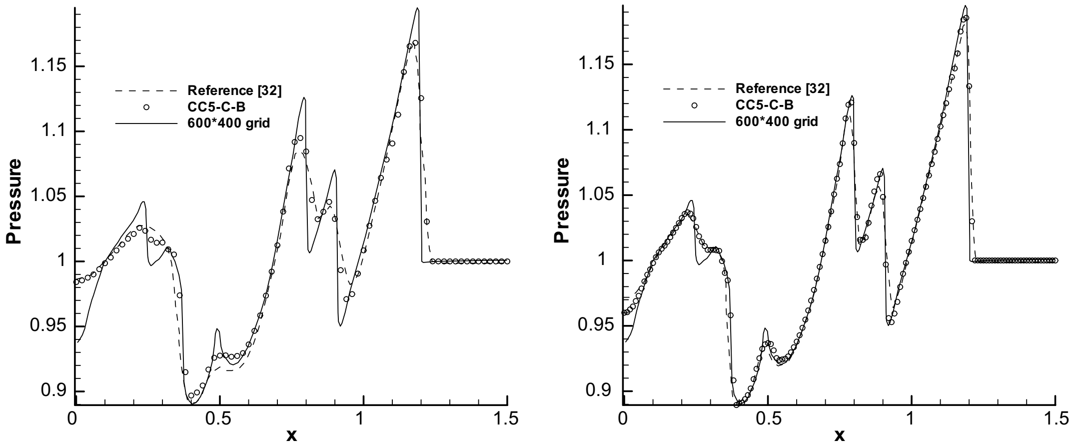

Fig. 15. Scatter plots of the pressure versus the distance from the z-axis in the plane $z = 0.4$. In the left picture the computational grid is $75 \times 75 \times 50$, while the right is $150 \times 150 \times 100$. The solid curves are the 2D solution computed by Langseth and LeVeque on a 600×400 grid.

4. Conclusions

A characteristic-based shock-capturing scheme has been formulated. Compactness, high-order accuracy and high resolution are achieved attribute to the characteristic-based method and the high-order compact algorithm. Without implementing of other shock-capturing schemes, the scheme possesses the advantages of linear compact schemes of spectral-like resolution, higher-order accuracy, and easy for boundary closure. The proposed algorithm has been shown to yield oscillation-free and high-order accurate results in our test cases.

Numerical tests in one-dimensional and multi-dimensional Euler system have been performed, and comparisons with some other high-order schemes have also been made. The following conclusions about the CC5-C-B scheme can be obtained:

- The presented characteristics-based method can effectively suppress non-physical oscillations;
- Sharper representations of discontinuities may be obtained by it with robustness than those by the ENO/WENO or compact-ENO/WENO schemes noted in articles of the references.
- The scheme shows good capacity in the resolution of small scale flow structures.

Acknowledgments

This work was supported by the *National Science Foundation of China* under the *Grant number* of 10321002 and 90205010. The authors are grateful to Professor Qing Shen for his help on our English.

References

[1] S. Pirozzoli, Conservative hybrid compact-WENO schemes for shock–turbulence interaction, J. Comput. Phys. 178 (2001) 81–117.
[2] R.S. Hirsh, High order accurate difference solutions of fluid mechanics problems by a compact differencing technique, J. Comput. Phys. 19 (1975) 90–109.
[3] S.K. Lele, Compact finite difference schemes with spectral-like resolution, J. Comput. Phys. 103 (1992) 16–42.
[4] D.X. Fu, Y.W. Ma, Analysis of super compact finite difference method and application to simulation of vortex–shock interaction, Int. J. Numer. Meth. Fluids 36 (7) (2001) 773–805.
[5] N.A. Adams, K. Shariff, A high-resolution hybrid compact-ENO scheme for shock–turbulence interaction problems, J. Comput. Phys. 127 (1996) 27–51.
[6] A.I. Tlstykh, M.V. Lipavskii, On performance of methods with third- and fifth-order compact upwind differencing, J. Comput. Phys. 140 (1998) 205–232.

[7] M. Zhuang, R.F. Cheng, Optimized upwind dispersion-relation-preserving finite difference scheme for computational aeroacoustics, AIAA J. 36 (11) (1998) 2146–2148.
[8] P.C. Chu, C. Fan, Sixth-order difference scheme for sigma coordinate ocean models, J. Phys. Oceanogr. 27 (9) (1997) 2064–2071.
[9] K. Mahesh, A family of high order finite difference schemes with good spectral resolution, J. Comput. Phys. 145 (1998) 332–358.
[10] D. Gaitonde, J.S. Shang, Optimized compact-difference-based finite-volume schemes for linear wave phenomena, J. Comput. Phys. 138 (1997) 617–643.
[11] M.H. Kobayashi, On a class of Padé finite volume methods, J. Comput. Phys. 156 (1999) 137–180.
[12] V. Daru, C. Tenaud, High order one-step monotonicity-preserving schemes for unsteady compressible flow calculations, J. Comput. Phys. 193 (2004) 563–594.
[13] B. Cockburn, C.-W. Shu, Nonlinearly stable compact schemes for shock calculation, SIAM J. Numer. Anal. 31 (3) (1994) 607–627.
[14] H.C. Yee, Explicit and implicit multidimensional compact high-resolution shock-capturing methods: formulation, J. Comput. Phys. 131 (1997) 216–232.
[15] K.S. Ravichandran, Higher order KFVS algorithms using compact upwind differenced operators, J. Comput. Phys. 130 (1997) 161–173.
[16] X. Deng, H. Zhang, Developing high-order weighted compact nonlinear schemes, J. Comput. Phys. 165 (2000) 22–44.
[17] X. Deng, H. Maekawa, Compact high-order accurate nonlinear schemes, J. Comput. Phys. 130 (1997) 77–91.
[18] A. Lerat, C. Corre, A residual-based compact schemes for the compressible Navier–Stokes equations, J. Comput. Phys. 170 (2001) 642–675.
[19] Y. Ma, D. Fu, Fourth order accurate compact scheme with group velocity control (GVC). Science in China, Series A: Mathematics, Physics, Astronomy 44 (9) (2001) 1197–1204.
[20] A. Harten, B. Engquist, S. Osher, S. Chakravarthy, Uniformly high order essentially accurate non-oscillatory schemes, III, J. Comput. Phys. 71 (1987) 231–303.
[21] C.-W. Shu, S. Osher, Efficient implementation of essentially non-oscillatory shock capturing schemes, J. Comput. Phys. 77 (1988) 439–471.
[22] C.-W. Shu, S. Osher, Efficient implementation of essentially non-oscillatory shock capturing schemes II, J. Comput. Phys. 83 (1989) 32–78.
[23] C.-W. Shu, Essentially non-oscillatory and weighted essentially non-oscillatory schemes for hyperbolic conservation laws, NASA/CR-97-206253, 1997.
[24] D.J. Hill, D.I. Pullin, Hybrid tuned center-difference-WENO method for large eddy simulations in the presence of strong shocks, J. Comput. Phys. 194 (2004) 435–450.
[25] Y.-X. Ren, M. Liu, H. Zhang, A characteristic-wise hybrid compact-WENO schemes for solving hyperbolic conservations, J. Comput. Phys. 192 (2003) 365–386.
[26] V.A. Titarev, E.F. Toro, ADER: arbitrary high order Godunov approach, J. Sci. Comput. 17 (1–4) (2002) 609–618.
[27] G.H. Tu, X.-J. Yuan, Z.-Q. Xia, et al., A class of compact upwind TVD difference schemes, Appl. Math. Mech. 27 (6) (2006) 765–772.
[28] G.-S. Jiang, C.-W. Shu, Efficient implementation of weighted ENO schemes, J. Comput. Phys. 126 (1996) 202–228.
[29] D. Levy, G. Puppo, G. Russo, A fourth-order central WENO scheme for multidimensional hyperbolic systems of conservation law, SIAM J. Sci. Comput. 24 (2) (2002) 480–506.
[30] Z. Wang, G.P. Huang, An essentially nonoscillatory high-order Padé-type (ENO-Padé) scheme, J. Comput. Phys. 177 (2002) 37–58.
[31] P. Woodward, P. Collela, The numerical simulation of two-dimensional fluid flow with strong shocks, J. Comput. Phys. 54 (1984) 115–173.
[32] J.O. Langseth, R.J. LeVeque, A wave propagation method for three-dimensional hyperbolic conservation laws, J. Comput. Phys. 165 (2000) 126–166.